Appl. Phys. B 40, 157–164 (1986)

Applied Physics B Photophysics and Laser Chemistry

Fluctuation Mechanism and Statistical Characteristics of Active-Passive Mode Locking in Giant Pulse Solid-State Lasers

Y. C. Yao and Z. G. Zhang

Department of Applied Physics, Beijing Polytechnic University, Beijing 100022, People's Republic of China

Received 6 November 1985/Accepted 8 March 1986

Abstract. A theoretical investigation of active-passive mode-locked lasers is presented. The main conclusion is that the intrinsic instability of a passively mode-locked laser due to the primordial noise fluctuation can be minimized by introducing an active modulator into the resonant cavity. Good agreement between computer simulation and experimental results reported previously is obtained.

PACS: 42.55

In spite of the fact that the passively mode-locked solid-state lasers are now in wide-spread use in a graet variety of applications, the realization of a reliable mode-locked operation can still be surprisingly troublesome [1]. The problems which have plagued the users include unreliable mode locking, multiple pulse train mode locking, irreproducible pulse train envelopes, large shot-to-shot variation in pulse width and relatively low peak-to-background contrast ratio. Even if every effort is made to minimize unstable technical factors, these problems cannot be overcome, owing to the stochastic nature of the mode-locking process.

The fluctuation model of passively mode-locking pulsed lasers first formulated by Letokhov [2] has been studied by a number of authors [1, 3–7]. It was found that under the same operating parameters (i. e., gain coefficient and spectral width of the gain medium, absorption characteristics of the saturable absorber, linear losses of the cavity and pumping intensity, etc.) the output parameters (amplitude and duration of the output pulses) may vary from shot by shot. Sometimes mode locking may not occur at all. Computer simulation of the evolution of a mode-locked pulse in a passively mode-locked laser shows that the amplitude and duration of the output pulses are not uniquely determined by the operating parameters of the system, but are distributed over relatively wide spreads according to their own statistical characteristics. It means that a purely passive mode-locked laser with a nonlinear absorber for both Q-switcher and mode-locker always has stochastic features.

Quite apart from the instability due to mechanical, thermal, optical, electrical and other technical causes, the pulse parameters vary by themselves. The probability distributions of pulse parameters are governed by the initial noise fluctuation and then by the nonlinear mode-locking system which transforms the initial noise into a sequence of ultrashort pulses. A number of successful active-passive mode-locking experiments [8–12] indicate that the statistical output characteristics can be greatly improved by simple modification of the mode-locking system.

The present work attempts to give a preliminary analysis of the evolution of the mode-locked pulse in an active-passive mode-locking system. A physical interpretation based on the fluctuation model is given at first, and then a computer simulation is made. Important results agreeing with experimental observations are revealed.

1. Mathematical Formulation and Physical Considerations

Consider a ring-type laser with gain and linear loss elements uniformly distributed throughout the cavity. It is identical to the model previously described by New [1] with the exception of an intracavity modulator. The saturable absorber is treated as sufficiently fast and sufficiently thin in comparison with the spatial width of a typical noise fluctuation.

The rate equation for the amplitude of n^{th} fluctuation in the cavity noise pattern is now of the form

$$\frac{du_n}{dk} = u_n\left(\bar{A} - \frac{B_u}{1+u_n} - \Gamma - \delta \sin^2 \omega t_n\right). \tag{1}$$

Here u_n is the intensity of n^{th} fluctuation peak, k is defined as $t=kT$, T is the cavity transit time, $\bar{A}$ is the gain coefficient averaged over the cavity, B_u and Γ are unsaturated absorption coefficient of the absorber and linear loss coefficient (all per cavity transit), respectively, δ is the modulation depth, ω is the sound frequency of the acousto-optic modulator, and t_n denotes the instant at which the n^{th} fluctuation passes through the modulator. All intensities are expressed in photon flux and normalized to the dye saturation intensity.

During the nonlinear stage the laser gain falls as a result of gain saturation, the average gain coefficient change per transit is given by

$$\frac{d\bar{A}}{dk} = -\frac{\bar{u}\bar{A}}{U}, \tag{2}$$

$$U = (T_{1b}\sigma_b)/(T\sigma_a), \tag{3}$$

where T_{1b} is the relaxation time of the absorber, σ_a and σ_b are the respective transition cross sections of the gain and absorbing media. The parameter $\bar{u}$ in (2) is the mean intensity of the complete signal profile. Considering the signal as a sequence of N Gaussian fluctuations whose durations (FWHM) are τ_n, then

$$\bar{u} = \pi^{1/2} \sum_{n=1}^{N} (u_n \tau_n)/T\alpha, \tag{4}$$

where $\alpha = 2(\ln 2)^{1/2}$.

Equations (1–4) have been discussed by various authors [1, 3–4], for the case of passive mode locking.

The expression in the parentheses on the right side of (1) is the net gain coefficient for n^{th} fluctuation, and is denoted by

$$G_n = \bar{A} - B - \Gamma - \delta \sin^2 \omega t_n, \tag{5}$$

where

$$B = B_u/(1+u_n). \tag{6}$$

In the linear stage of signal evolution, both the gain and absorbing media are unsaturated, so that the average gain coefficient $\bar{A}$ and absorption coefficient B may be replaced by their unsaturated values A_u and B_u, then the width of the modulation window can be defined as

$$W = 2(1/\omega) \arcsin(G_u/\delta)^{1/2}, \tag{7}$$

where G_u is the unsaturated net gain coefficient in the absence of an intracavity modulator, and is given by

$$G_u = A_u - B_u - \Gamma. \tag{8}$$

To see what happens in the linear stage, we can easily imagine that the fluctuations inside the window experience gain and will evolve gradually, while the fluctuations outside the window experience loss and hence gradually decay. At the same time, since the modulation loss is in the shape of a sinusoid, the fluctuations near the center of the window acquire more gain and will grow faster, while the fluctuations near the border of the window acquire less gain and evolve slower. Irrespective of the initial noise pattern, the modulator always gives preference to the peaks near the center and discriminates against those near the border. Integrating (1) over the entire linear stage and assuming that the small-signal gain coefficient A_u remains constant, the peak intensity of the n^{th} fluctuation at the end of the linear stage would be of the form

$$\begin{aligned} u_n(k_{\text{lin}}) &= u_n(0) \exp(G_u k_{\text{lin}}) \exp(-k_{\text{lin}} \delta \sin^2 \omega t_n) \\ &= u_{np} \exp(-k_{\text{lin}} \delta \sin^2 \omega t_n), \end{aligned} \tag{9}$$

where $u_{np} = u_n(0) \exp(G_u k_{\text{lin}})$ is obviously the peak intensity of n^{th} fluctuation at the end of the linear stage in the case of purely passive mode locking, and k_{lin} is the number of transits of the linear stage. Equation (9) shows that the number of fluctuations in the space-time domain will be greatly reduced after a large number of linear transits owing to the effect of active modulation.

The nonlinear stage is characterized by the saturation of dye absorption and/or laser gain. As the fluctuations grow, the gain $\bar{A}$ will decrease, so that the window will become narrower; on the other hand, as a result of absorption saturation, large peaks will make some "holes" in the loss curve, as shown in Fig. 1b, and the effect of gain saturation may be counteracted. Once these two actions balance with each other, the peak u_n will be removed from the window and will begin to decay during the next transit, and thereafter.

Whether the absorption saturation can balance out the effect of gain saturation depends not only on the magnitude of u_n (say the depth of the hole), but also on the location of the peak. Obviously, the net gain G_n of the peaks near the center of the window is always

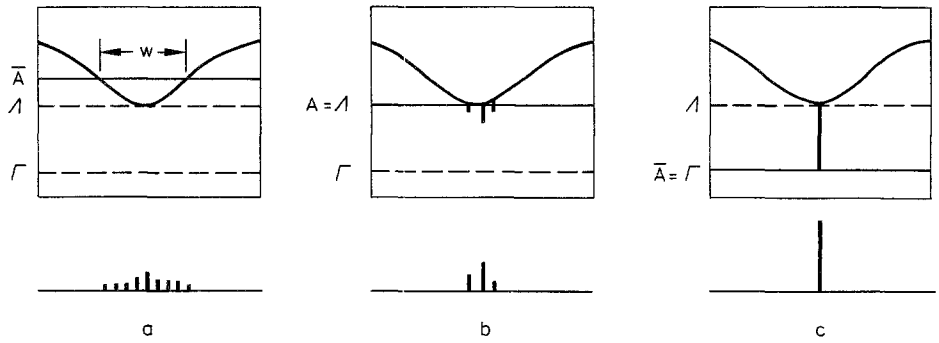

Fig. 1. (a) Modulation window and noise fluctuations at the end of linear stage. (b) Evolution of pulses in nonlinear stage. (c) Formation of giant pulse

positive before the average gain $\bar{A}$ has fallen to $\Lambda(=B_u+\Gamma)$, while for the peaks near the border, only those which have sufficient intensity can counteract the gain saturation. In fact, after numbers of linear transits the peaks on both sides would inevitably be weaker than those near the window center; they are incapable of resisting the narrowing effect caused by gain saturation, and will ultimately be eliminated. When $\bar{A}=\Lambda$, the width of the window almost becomes zero, and only one or very few peaks will remain in the window. This moment is defined as the beginning of the giant pulse stage. The competition between the largest peak and the other peaks, if any, goes on until the weaker peaks completely die out. The largest peak continues to grow until $\bar{A}=\Gamma$, at which point it reaches the intensity maximum (Fig. 1c) and then attenuates according to the cavity loss.

The compression effect of the active modulator on the pulse duration can be estimated as follows:

Consider a sequence of Gaussian fluctuations whose durations are τ_n, then the instantaneous intensity of the n^{th} fluctuation can be written as

$$\cdot\ u_n(t')=u_n\exp(-\alpha^2 t'^2/\tau_n^2)\,. \tag{10}$$

Taking $t'=\tau_n/2$, we get

$$\frac{d\ln\tau_n}{dk}=\frac{2}{\alpha^2}\left(\frac{du_n(t')}{dk}\bigg|_{t'=\frac{1}{2}\tau_n}-\frac{d\ln u_n}{dk}\right). \tag{11}$$

Assuming that the response of the saturable absorber is sufficiently fast compared with the instantaneous variation of the pulse intensity, then (1) can be written as

$$\frac{d\ln u_n(t')}{dk}=\bar{A}-\frac{B_u}{1+u_n(t')}-\Gamma-\delta\sin^2\omega(t_n+t')\,. \tag{12}$$

When $t'=\tau_n/2$, $u_n(t')=u_n/2$, then

$$\frac{d\ln u_n(t')}{dk}\bigg|_{t'=\frac{1}{2}\tau_n}=\bar{A}-\frac{B_u}{1+u_n/2}-\Gamma-\delta\sin^2\omega(t_n\pm\tau_n/2)\,. \tag{13}$$

From (11 and 13) we obtain the respective equations for the compression on the fron and trailing edges of n^{th} pulse

$$\frac{d\ln\tau_n^-}{dk}=-2(1/\alpha^2)\,(\beta+\gamma_-)\,, \tag{14a}$$

$$\frac{d\ln\tau_n^+}{dk}=-2(1/\alpha^2)\,(\beta+\gamma_+)\,, \tag{14b}$$

where

$$\beta=(B_u u_n/2)/[(1+u_n)\,(1+u_n/2)]\,, \tag{15a}$$

$$\gamma_-=\delta\sin^2\omega(t_n-\tau_{n,k}/2)-\delta\sin^2\omega t_n\,, \tag{15b}$$

$$\gamma_+=\delta\sin^2\omega(t_n+\tau_{n,k}/2)-\delta\sin^2\omega t_n\,. \tag{15c}$$

Defining the pulse width τ_n as the arithmetic mean of τ_n^- and τ_n^+, from (14a and b) we obtain the width of the n^{th} pulse after $(k+1)$ nonlinear passes

$$\tau_{n,k+1}=\tfrac{1}{2}\exp(-2/\alpha^2)\,[\tau_{n,k}^-\exp(-2\gamma_-/\alpha^2)+\tau_{n,k}^+\exp(-2\gamma_+/\alpha^2)]\,. \tag{16}$$

Consider the pulse which is situated in the center of the modulation window (i.e., $\omega t_n=k\pi$, k: integer). From (15b and c) we have

$$\gamma=\gamma_-=\gamma_+=\delta\sin^2(\omega\tau_n/2)\,. \tag{17}$$

Equation (16) becomes

$$\tau_{n,k+1}=\eta\exp(-2\beta/\alpha^2)_{n,k}\,, \tag{18}$$

where $\eta=\exp(-2\gamma/\alpha^2)$ is the compression factor (per pass) coming from the active modulator, and the factor $\exp(-2\beta/\alpha^2)$ is the compression factor coming from the nonlinear absorber.

Consider a laser having a cavity transit time $T=6$ ns, an initial absorption coefficient $B_u=0.75$, a modulation depth $\delta=0.6$ and an initial pulse width $\tau_n=100$ ps. In this case, $\eta=0.9997$ but $\exp(-2\beta/\alpha^2)=0.914$. Thus we can see that the modu-

lator has very little effect on the pulse width during the nonlinear stage.

If the pulse lies away from the window center, for example, on the right side of the window, then $\gamma_- < 0$ and $\gamma_+ > 0$, the front edge will be expanded and the trailing edge will be compressed. But the total effect, as it is estimated above, is negligible.

2. Simulation Results

In principle, the statistical behavior of the mode-locked pulses can be obtained by solving (1 and 2) for N fluctuations in the noise pattern ($N+1$ simultaneous equations) and finding the related probabilities in a large number of shots. It is straightforward to do this by means of numerical simulation.

Integrating (1 and 2) and assuming that the average gain $\bar{A}$ remains constant during each pass, we have

$$\ln u_{n,k+1} = \ln u_{n,k} + [\bar{A}_k - B_u/(1+u_{n,k}) - \Gamma - \delta \sin^2 \omega t_n], \tag{19}$$

$$\ln \bar{A}_{k+1} = \ln \bar{A}_k - \bar{u}_k/U. \tag{20}$$

Equations (19 and 20) have been computed iteratively for every pass and every fluctuation from the beginning of the nonlinear stage until the net gain G_n of the largest fluctuation falls to zero.

As indicated by (9), the peak intensities at the beginning of the nonlinear stage are

$$u_n = u_{np} \exp(-k_{\text{lin}} \delta \sin^2 \omega t_n),$$

where u_{np} is the peak intensity of the n^{th} fluctuation at the beginning of the nonlinear stage in the case of purely passive mode-locking and k_{lin} is the number of passes of the linear stage. N values of u_{np} can be generated by the computer as has been done in [1]. The length of the linear stage in the case of active-passive mode-locking would be slightly longer than that of parely passive case owing to the additional modulation loss. However, we let the number of linear transits be equal to that of the purely passive case [1], for convenience;

$$k_{\text{lin}} = 3.53\, p^{-1/4} (K/\Lambda)^{1/2}. \tag{21}$$

In so doing, sufficiently good results can be obtained, as will be seen later. We have reason to expect that the actual results are even better. Moreover, all fluctuations are assumed to have the same duration at the outset. Thus we can obtain the initial distribution of u_n in (9), making use of (21) and u_{np} obtained as above.

Finally, the average gain coefficient $\bar{A}_k$ in (19) decreases as the number of nonlinear passes k increases according to (20). The initial value of $\bar{A}_k$ equals $A_u = G_u + \Lambda$. The dependence of G_u on the pumping intensity is given by [1]

$$G_u = 11.7\, p^{1/4} (\Lambda/K)^{1/2}. \tag{22}$$

Typical parameters of the laser system can now be inserted into the above equations to perform the computer program. In order to compare the results with what have been obtained in the purely passive case [1], we take $T = 6$ ns, $M = 1080$ (gain bandwidth: 1.8×10^{11} Hz), $T_{\text{amp}} = 125\ \mu s$, $\Gamma = 0.5$, $T_{1b} = 10$ ps, $\sigma_b = 8 \times 10^{-16}$ cm^2, $\sigma_a = 2.13 \times 10^{-19}$ cm^2. The relative pumping energy P, initial absorption coefficient B_u and the modulation depth δ are taken to be variable parameters.

2.1. Mode-Locking Probability and Threshold Characteristics

Following the suggestion of New [1] we utilize the parameter E as a measure of the mode-locking quality. E is defined as the percentage of total energy ultimately contained in the largest fluctuation. Assuming that all fluctuations are Gaussian in shape, we can obtain

$$E = (u_{1f} \tau_{1f}) \Big/ \left(\sum_{n=1}^{N} u_{nf} \tau_{nf} \right). \tag{23}$$

Here u_{nf} and τ_{nf} are the ultimate peak intensity and ultimate width of the n^{th} fluctuation, respectively, and the latter can be found from (26) below. The subscript 1 refers to the largest fluctuation. Table 1 shows the summary of the results for sequences of 100 computer shots for three values of P with $B_u = 0.75$ and $\delta = 0$ (purely passive mode-locking).

We see from Table 1 that an increase of 14% in pumping energy will be needed to raise the mode-locking probability from 80% to 100%. This means that the threshold characteristic is rather flat. However, a dramatic change will occur once the modulation is applied. Table 2 shows the performance summary for sequences of 100 computer shots for three values of modulation depth with $B_u = 0.75$, $P = 1.10$.

It can be seen from Table 2 that the mode-locking probability immediately increases to 100% provided a small amount of modulation is applied. This means

Table 1

Relative pumping energy	Mode-looking probability [%]	$E > 98\%$	$E > 90\%$	$30\% < E < 90\%$
$P = 1.06$	80	74	77	3
$P = 1.10$	95	82	88	7
$P = 1.21$	100	64	74	26

Table 2

Modulation depth	Mode-locking probability [%]	$E>99\%$	$E>98\%$	$E>90\%$	$50\%<E<90\%$
$\delta=0.2$	100	89	90	97	3
$\delta=0.4$	100	97	97	99	1
$\delta=0.6$	100	100	100	100	0

that in the active-passive case the separation between the laser threshold and the mode-locking threshold become narrower because the mode-locking threshold lowers remarkably, that is to say, the threshold characteristic becomes very sharp.

The statistic nature of the mode-locking threshold of purely passive mode-locking was investigated experimentally by Lü et al. [13]. It was demonstrated that the sharpness of the threshold can be estimated from the semi-empirical formula given by New [1].

$$X=(G_u B_u U R)/(\Lambda+G_u)>X_Q\,, \tag{24}$$

where X_Q is determined empirically. Its value ranges typically from 0.65 to 0.7. For a laser with fixed parameter values, whether condition (24) can be satisfied will depend on the value of G_u and R. According to (22), we have $G_u=0.035$ with $P=1.06$ and other parameters are such as above. From (24) we obtain $R>4.05$. However, for a purely passive mode-locking system with parameters as given above, the statistical variable R is distributed over the range of 3 to 10 (as shown in Fig. 2, where $r=u_{1i}/u_{2i}$ is the ratio of the largest to the second largest peaks at the beginning of the nonlinear stage). Of course, we may control G_u, namely P, to satisfy (24) even if $R=3$. In this way, we find from (24 and 22) that the minimum pumping energy required to achieve 100% mode locking is $P=1.16$ (16% above laser threshold).

In active-passive systems, the modulator profoundly influences the distributions of R and r. The values of R are no less than 15 as shown in Fig. 2b and c. Hence condition (24) can easily be satisfied even for a small value of G_u. Assuming that the minimum value of R in the case of active-passive mode-locking is four times as large as that of purely passive case, then G_u will become near one-fourth of that in the case of purely passive mode-locking. It can be found from (22) that the minimum pumping energy required to achieve 100% mode locking will then reduce to $P=1.001$ (0.1% above laser threshold). That is to say, the mode-locking threshold nearly coincides with the laser threshold.

2.2. *Mode-Locking Quality and Amplitude Stability*

Table 1 shows that an increase in mode-locking probability is accompanied by an increase in multiple pulse-train probability. Thus, as a whole, the output pulses of a purely passive mode-locking system are poor in stability. In the case of active-passive mode-locking, however, this problem will be greatly alleviated, as has been shown in Table 2.

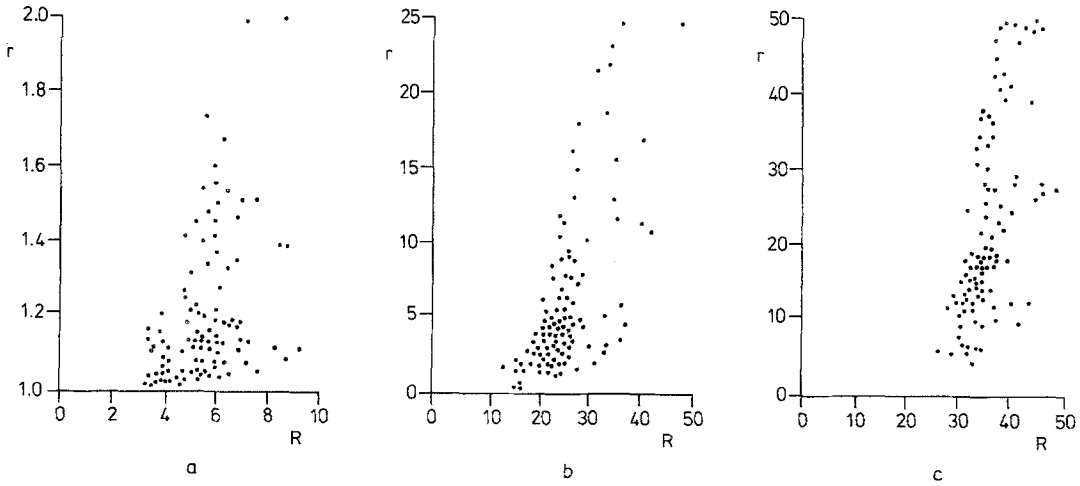

Fig. 2a–c. $R-r$ plane of 100 computer shots. (a) Passive mode locking with $P=1.06$, $B_u=0.75$. (b) and (c) Active-passive mode locking with $P=1.10$, $B_u=0.75$; (b) $\delta=0.2$, (c) $\delta=0.6$

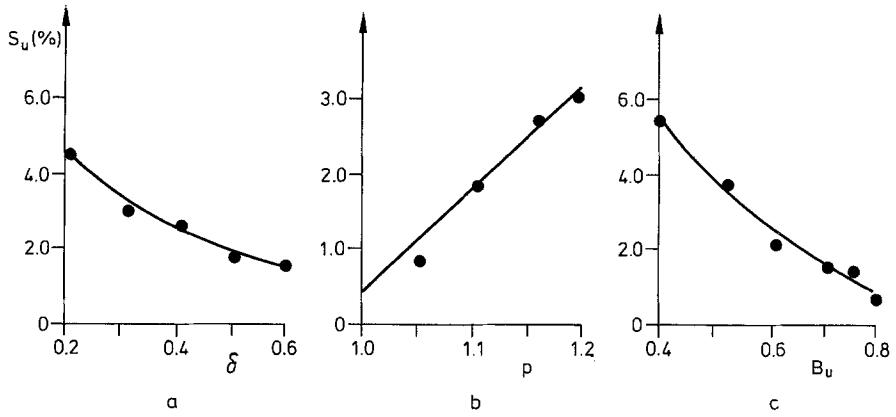

Fig. 3a–c. Variation of amplitude stability for sequences of 100 computer shots with respect to various operating parameters. (a) Stability versus modulation depth ($B_u=0.75$, $P=1.10$). (b) Stability versus relative pumping energy ($\delta=0.6$, $B_u=0.75$). (c) Stability versus unbleached absorption coefficient ($P=1.10$, $\delta=0.6$)

As we may expect from the preceding discussion, the distributions of R and r can be controlled by varying the depth of modulation. An increase in modulation depth results in an increase not only in R but also in r. The increase in r will lead to an effective reduction in multiple pulse-train probability. For example, three shots in Fig. 2b with $r<1.10$ correspond to three shots in Table 2 where $50\%<E<90\%$. Their E's (as a measure of double pulse-train, parameter $\mathscr{E}$ is defined as the ratio of the ultimate peak intensity of the largest fluctuation to that of the second largest fluctuation, i.e., $\mathscr{E}=u_{1f}/u_{2f}$) are all less than 2. This indicates the appearance of double-pulse trains. As the modulation depth is increased to 0.6, all values of r exceed 2.3, all values of $\mathscr{E}$ exceed 10^4 and all $\mathscr{E}$'s exceed 99%. It indicates that hundred percent mode locking has been achieved without multiple pulse train.

The amplitude stability can be defined as the mean coefficient of dispersion of the statistical variable u_{1f}

$$S_u=\langle|\Delta u_{1f}|\rangle/\langle u_{1f}\rangle\,, \tag{25}$$

where $\langle u_{1f}\rangle$ is the arithmetic mean of the ultimate mode-locked pulse intensities in a large number of shots under the same operating conditions, $\langle|\Delta u_{1f}|\rangle$ is the mean deviation from the mean.

The amplitude stability S_u as a function of modulation depth is shown in Fig. 3a. Fig. 3b shows the variation of stability with pumping energy. Lowering the pumping energy P means an increase in number of linear transits, thus an increase in r. This is advantageous to the improvement in stability. Figure 3c shows the variation of amplitude stability with the unbleached absorption coefficient. Operating at higher B_u is conducive to the increase in discrimination ability of the system, hence to the improvement in stability.

2.3. *Pulse Width and Pulse-Width Stability*

In principle, duration of the mode-locked pulses can be computed iteratively from (16). However, it is more convenient to utilize the relation

$$\frac{\tau_{nf}}{\tau_{ni}}=\left(\frac{(1+u_{nf})\,[Y_n+u_{ni}(1+Y_n)]}{(1+u_{ni})\,[Y_n+u_{nf}(1+Y_n)]}\right)^{1/2}, \tag{26}$$

where

$$Y_n=(A_u-B_u-\Gamma-\delta\sin^2\omega t_n)/B_u\,. \tag{27}$$

All fluctuations are assumed to have the same duration at the outset. Using (4), we have

$$\tau_i=\alpha\bar{u}T\Big/\left(\pi^{1/2}\sum_{n=1}^{N}u_n\right). \tag{28}$$

Figure 4 shows the distributions of the ultimate mode-locked pulse durations in both purely passive and active-passive cases. It can be seen from Fig. 4a that the pulse durations are dispersed shot by shot over a relative wide spread as $\delta=0$. This has been verified experimentally by Bechtel and Smith [14] and theoretically by New [1]. Figure 4b shows that in the case of active-passive mode-locking, all pulse widths merge together into a small range, that is to say, the pulse width is rather stable.

It can be seen from Fig. 4 that the pulse widths of an active-passive system are, for the most part, somewhat greater than those of a passive system under the same operating conditions. To explain this, we rewrite (26) in the form

$$\left(\frac{\tau_{nf}}{\tau_{ni}}\right)^2=\left(\frac{Y_n+u_{ni}(1+Y_n)}{1+u_{ni}}\right)\left(\frac{1+u_{nf}}{Y_n+u_{nf}(1+Y_n)}\right)$$
$$=F(u_{ni})G(u_{nf})\,, \tag{29}$$

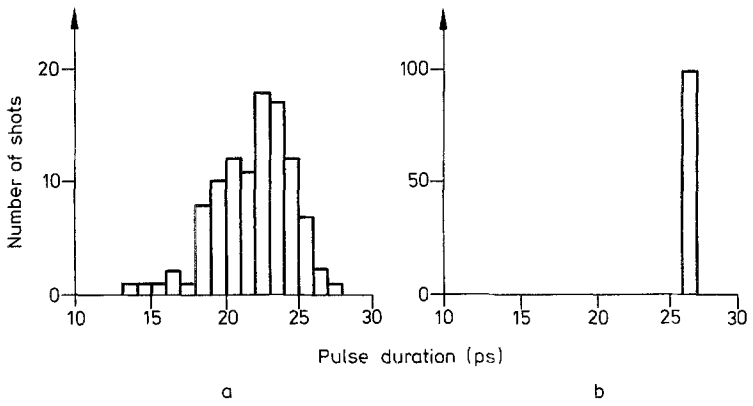

Fig. 4a and b. Histograms showing the spreads of the ultimate mode-locked pulse durations. (a) 95 successful shots from 100-shot computer run with $P=1.10$, $B_u=0.75$ and $\delta=0$. (b) 100 computer shots with $P=1.10$, $B_u=0.75$ and $\delta=0.6$

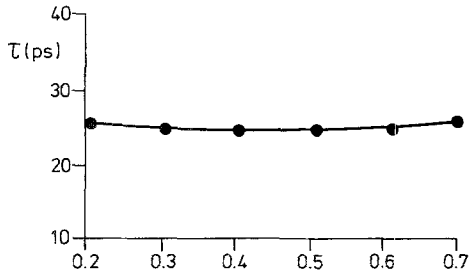

Fig. 5. Pulse width as a function of modulation depth with $P=1.10$ and $B_u=0.75$

where the ultimate normalized intensity of the largest fluctuation $u_{1f} \gg 1$. Because $Y_1 \ll 1$, we get

$$G(u_{1f}) = \frac{1+u_{1f}}{Y_1+u_{1f}(1+Y_1)} \simeq 1 .$$

As $u_{1i} \ll 1$, we obtain the following expression for the change $dF(u_{1i})$ due to the intensity variation du_{1i}

$$\frac{dF(u_{1i})}{F(u_{1i})} = \frac{du_{1i}}{u_{1i}(1+u_{1i})} \simeq \frac{du_{1i}}{u_{1i}} .$$

If, for example, u_{1i} increases by 10%, the pulse width will increase by 5%. As has been said before, at the end of the linear stage, the values of R of the active-passive system are much greater than those of the passive one. For the same $\bar{u}$, the active-passive system will have a greater u_{1i} which will cause the pulses to broaden. This effect will be sufficient to counteract the compression effect of the modulator mentioned in Sect. 1. For the same reason, an increase in modulation depth will result in an increase in pulse width, as shown in Fig. 5.

Pulse-width stability is defined by

$$S_\tau = \langle |\Delta\tau_{1f}| \rangle / \langle \tau_{1f} \rangle . \tag{30}$$

Variations of pulse-width stability with respect to various operating parameters are shown in Fig. 6.

2.4. Pulse Energy

The energy density of the mode-locked pulse is given by

$$E_1 = (\pi^{1/2} u_{1f} \tau_{1f} h\nu)/(\alpha \sigma_b T_{1b}) , \tag{31}$$

where $h\nu = 1.87 \times 10^{-19}$ Joules for $\lambda = 1.06$ μm. With $P=1.06$, $B_u=0.75$, $\delta=0.2$ other parameters are the same as above, and beam diameter is assumed to be 1 mm, we find from (31) that the pulse energy is approximately 1.8 mJ (inside the cavity). This value is almost twice the average pulse energy of a passive mode-locking system under the same conditions. The energy enhancement can be attributed to the modu-

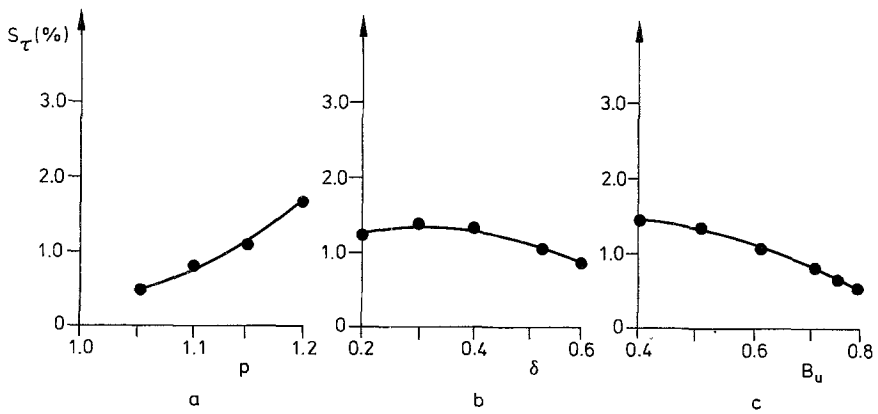

Fig. 6a–c. Pulse-width stability for sequences of 100 computer shots. (a) Stability versus relative pumping energy ($B_u=0.75$, $\delta=0.6$). (b) Stability versus modulation depth ($P=1.10$, $B_u=0.75$). (c) Stability versus unbleached absorption coefficient ($P=1.10$, $\delta=0.6$)

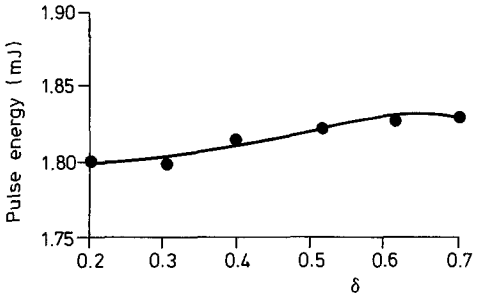

Fig. 7. Dependence of the pulse energy on the modulation depth with $P=1.06$ and $B_u=0.75$

lator which condenses the background energy into the mode-locked pulse and effectively shortens the nonlinear process. The amount of increase depends apparently on the type of modulation. The pulse energy increases slightly as the modulation depth is increased at low modulation depths, after passing a maximum, it falls off slightly for higher modulation depths. The computed curve is shown in Fig. 7.

3. Conclusions

The function of the mode-locking system is merely to transform the initial noise distribution into a desirable distribution (a stable mode-locked pulse with extremely weak background). Thus, the statistical characteristics of the mode-locked pulses can be greatly improved by appropriate modification of the mode-locking system. Computer simulation shows the remarkable improvements in performance including 100% mode-locking probability without satellite, a very sharp mode-locking threshold, high pulse-amplitude and pulse-width stabilities, better peak-to-background contrast, and a considerable increase in pulse energy. These can be achieved by introducing an active modulator into the cavity of a passive mode-locking system. The analysis is based upon the fluctuation model. The effect of linear amplification of the passive part and the influence of the modulator on the distribution of the noise fluctuation are treated separately according to (9). The modulation loss in (1) may be different for different type of modulation, but the effect is essentially the same.

References

1. G.H.C. New: Proc. IEEE **67**, 380–396 (1979)
2. V.S. Letokhov: Sov. Phys. JETP **28**, 562–568 (1969)
3. T.I. Kuznetsova: Sov. Phys. JETP **30**, 904–909 (1970)
4. P.G. Kryukov, V.S. Letokhov: IEEE J. QE-**8**, 766–782 (1972)
5. W.H. Glenn: IEEE J. QE-**11**, 8–17 (1975)
6. R. Wilbrandt, H. Weber: IEEE J. QE-**11**, 186–190 (1975)
7. A. Leitner, M.E. Lippitsch, E. Roschger, F.R. Aussenegg: IEEE J. QE-**19**, 562–566 (1983)
8. S. Kishida, T. Yamane: Opt. Commun **18**, 19–20 (1976)
9. W. Seka, J. Bunkenburg: J. Appl. Phys. **49**, 2277–2280 (1978)
10. G.F. Albrecht, J. Bunkenburg: Opt. Commun. **38**, 377–380 (1981)
11. M.A. Lewis, J.T. Knudtson: Appl. Opt. **21**, 2897–2900 (1982)
12. H.P. Kortz: IEEE J. QE-**19**, 578–584 (1983)
13. B. Lü, W. Rudolph, H. Weber: Opt. Commun **53**, 203–209 (1985)
14. J.H. Bechtel, W.L. Smith: Phys. Lett. **55A**, 203–204 (1975)